

## Variations in organic aerosol optical and hygroscopic properties upon heterogeneous OH oxidation

Christopher D. Cappa,<sup>1</sup> Daphne L. Che,<sup>2,3</sup> Sean H. Kessler,<sup>4</sup> Jesse H. Kroll,<sup>4,5</sup> and Kevin R. Wilson<sup>2</sup>

Received 5 March 2011; revised 29 April 2011; accepted 11 May 2011; published 6 August 2011.

[1] Measurements of the evolution of organic aerosol extinction cross sections ( $\sigma_{\text{ext}}$ ) and subsaturated hygroscopicity upon heterogeneous OH oxidation are reported for two model compounds, squalane (a C<sub>30</sub> saturated hydrocarbon) and azelaic acid (a C<sub>9</sub> dicarboxylic acid). For both compounds, the  $\sigma_{\text{ext}}$  values at 532 nm increase substantially as the particles undergo oxidation, exhibiting a logarithmic increase with OH exposure. The increase in  $\sigma_{\text{ext}}$  correlates with both an increase in the particle oxygen to carbon (O:C) atomic ratio and density and a decrease in mean molecular weight. The measurements have been used to calculate the variation with oxidation of the mean polarizability,  $\alpha$ , of the molecules comprising the particles. The absolute  $\alpha$  values for the two systems are shown to be related through the variation in the particle chemical composition, specifically the relative abundances of C, O, and H atoms and the mean molecular weight. Unlike  $\sigma_{\text{ext}}$ , it was found that the evolution of the particle hygroscopicity upon oxidation is quite different for the two model systems considered. Hygroscopicity was quantified by measuring  $\gamma_{\text{ext}}$ , which is a single-parameter representation of hygroscopicity that describes the increase in extinction upon exposure of the particles to a high–relative humidity environment (here, 75% and 85% RH). For unoxidized squalane,  $\gamma_{\text{ext}}$  was zero and only increased slowly as the particles were oxidized by OH radicals. In contrast,  $\gamma_{\text{ext}}$  for azelaic acid increased rapidly upon exposure to OH, eventually reaching a plateau at high OH exposures. In general,  $\gamma_{\text{ext}}$  appears to vary sigmoidally with O:C, reaching a plateau at high O:C.

**Citation:** Cappa, C. D., D. L. Che, S. H. Kessler, J. H. Kroll, and K. R. Wilson (2011), Variations in organic aerosol optical and hygroscopic properties upon heterogeneous OH oxidation, *J. Geophys. Res.*, 116, D15204, doi:10.1029/2011JD015918.

### 1. Introduction

[2] Atmospheric aerosols play a key role in determining the radiative balance of the Earth through their ability to both scatter and absorb solar radiation [*Intergovernmental Panel on Climate Change*, 2007]. Light extinction by aerosols is the sum of light scattering and absorption. The efficiency of light extinction by aerosols is a strong function of both particle size and chemical composition. The chemical composition of particles determines their complex refractive index, and the refractive index determines, in turn, their ability to interact with light of a given wavelength and thus their impacts on climate [*Kanakidou et al.*, 2005] and on

ozone formation through the reduction in surface UV radiation [*Dickerson et al.*, 1997; *Jacobson*, 1999].

[3] Atmospheric aerosols are composed of both inorganic and organic compounds, the composition of which varies greatly in both space and time [*Murphy et al.*, 2006; *Zhang et al.*, 2007]. The refractive index (RI) of many inorganic aerosol components (e.g., (NH<sub>4</sub>)SO<sub>4</sub>, NaCl) have been reasonably well established [e.g., *Abo Rizeq et al.*, 2007]. In contrast, the RI of organic aerosol has not been sufficiently characterized. In part, this is due to the much greater chemical complexity of the organic versus the inorganic fraction of atmospheric aerosols [*Kanakidou et al.*, 2005], but also results from there being a limited number of measurements until recently [*Schnaiter et al.*, 2003; *Barkey et al.*, 2007; *Yu et al.*, 2008; *Kim et al.*, 2010; *Lang-Yona et al.*, 2010; *Nakayama et al.*, 2010]. Of course, the inorganic and organic components are often internally mixed in ambient particles, but it is important that the organic fraction be studied independently as the sources of the inorganic and organic fractions are often distinct [*Dentener et al.*, 2006] and the relative abundances of the inorganic and organic components can vary greatly.

[4] It is necessary to establish a framework wherein the optical properties of organic aerosol are understood both in

<sup>1</sup>Department of Civil and Environmental Engineering, University of California, Davis, California, USA.

<sup>2</sup>Chemical Sciences Division, Lawrence Berkeley National Laboratory, Berkeley, California, USA.

<sup>3</sup>Now at Department of Chemistry, Stanford University, Stanford, California, USA.

<sup>4</sup>Department of Chemical Engineering, Massachusetts Institute of Technology, Cambridge, Massachusetts, USA.

<sup>5</sup>Also at Department of Civil and Environmental Engineering, Massachusetts Institute of Technology, Cambridge, Massachusetts, USA.

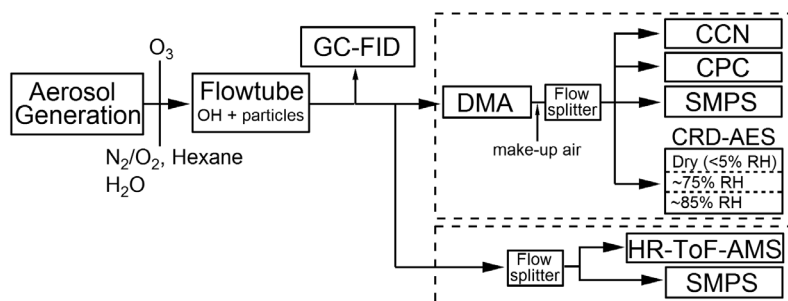


**Figure 1.** Schematic of the experimental setup. In one set of experiments, particles were reacted with OH in the flow tube, size selected with the DMA, and then characterized using the CRD-AES, an SMPS, CPC, and a CCN counter. In a second set of experiments, the particles were characterized using an HR-ToF-AMS and an SMPS.

terms of their different sources and how they may be altered by in situ chemical processing. One important question with respect to organic aerosol relates to what extent variations in particle composition correspond to variations in particle optical properties. This has implications for the understanding and representation of the optical properties of OA derived from different sources (e.g., primary versus secondary, biogenic versus anthropogenic) and the evolution of these properties as organic particles age in the atmosphere. The variability in organic aerosol (OA) sources, coupled with the observation that atmospheric OA composition is not static [e.g., Ng *et al.*, 2010], suggests that there may not be a single, well-defined refractive index that can be used to characterize OA; nonetheless, this is the approach currently taken by most models [Kinne *et al.*, 2003]. In this study, we present measurements that directly address the connection between composition and refractive index for two model organic systems.

[5] Additionally, the hygroscopicity of particles, or their ability to take up water, influences their ability to interact with solar radiation [e.g., Myhre *et al.*, 2004]. As water is taken up particles grow, causing them to scatter more light. At the same time, water generally has a smaller refractive index than either organic or inorganic aerosol components, and thus water uptake leads a decrease in the overall particle refractive index. The predominant inorganic aerosol components are generally very hygroscopic. In contrast, the hygroscopicity of organic aerosol components is highly variable, and may change as particles age in the atmosphere [Petters *et al.*, 2006; Jimenez *et al.*, 2009]. However, as with refractive index, most models assume a single subsaturated hygroscopic growth curve to describe organic aerosol water uptake [Kinne *et al.*, 2003].

[6] Here, we report on experiments wherein the evolution of the light extinction cross section and the hygroscopicity of two model organic compounds (squalane and azelaic acid) upon heterogeneous oxidation by OH radicals has been determined. A long-chain saturated hydrocarbon, squalane, was chosen as a surrogate for primary organic aerosol, while azelaic acid (O:C ratio of 0.44) has been observed in atmospheric aerosols [e.g., Fraser *et al.*, 2003] and is a reasonable proxy for oxidized organic aerosol [Jimenez *et al.*, 2009]. The results indicate that both the extinction cross section and the particle hygroscopicity increase as the particles are oxidized. The magnitude of the

observed increases in these bulk aerosol properties depends on the initial compound identity and is shown to be related to changes in the atomic composition, molecular volume and particle density.

## 2. Experimental Methods

[7] Particle heterogeneous OH oxidation experiments were conducted using the flow tube and methods described by Smith *et al.* [2009]. Particle light extinction was measured at 532 nm using a cavity ring-down aerosol extinction spectrometer (CRD-AES), described by Baynard *et al.* [2007]. Particle hygroscopicity was assessed by simultaneously measuring the change in extinction between dry particles (RH <5%) and particles exposed to and maintained at ~75% and ~85% relative humidity [Massoli *et al.*, 2009]. A schematic of the experimental setup is shown in Figure 1.

[8] In brief, lognormal distributions of pure squalane or azelaic acid particles were generated via homogeneous nucleation in a N<sub>2</sub> stream. The generated particles were mixed with O<sub>2</sub> (5% by volume), trace hexane and variable amounts of O<sub>3</sub>, and water vapor was maintained at 30% RH. The resulting mixture was passed through a 130 cm long, 2.5 cm diameter quartz flow tube. OH radicals were generated along the length of the flow tube using four Hg lamps ( $\lambda = 254$  nm). OH concentrations were controlled by varying the amount of O<sub>3</sub> present in the stream. Steady state OH concentrations were determined by measuring the loss of hexane through the flow tube when the lights were on using a gas chromatograph with flame ionization detection (GC-FID) as described by Smith *et al.* [2009]. The initial hexane concentration was ~100 ppb. The total flow rate through the flow tube was 1.0 lpm, corresponding to a reaction time of 37 s.

[9] Particles exiting the flow tube were size selected using a long differential mobility analyzer (DMA; TSI, Inc.). Following the size selection by the DMA, the aerosol stream was quantitatively distributed using an aerosol flow splitter to a condensation particle counter (CPC; TSI, Inc.), a scanning mobility particle sizer (SMPS; TSI, Inc.), a cloud condensation nuclei (CCN) counter (Droplet Measurement Technologies) and the CRD-AES. To ensure sufficient flow to each of the instruments, particle-free makeup air was added to the size-selected aerosol stream. Measurement of the size distribution of the size-selected aerosol allowed for

characterization of the fraction of doubly charged (and therefore different size) particles that passed through the DMA column. In a few experiments, the aerosol was doubly size selected to decrease the contribution of such doubly charged or “q2” particles. In most experiments, the q2 number fraction was kept below 5% although for some experiments it was as large as 15%. All extinction measurements were corrected for the contribution from q2 particles by calculating the extinction due to singly and doubly charged particles using spherical particle Mie theory [Bohren and Huffman, 1983], weighting by the measured particle number at each size, and multiplying the measured extinction by the ratio  $\sigma_{\text{ext,calc}}(q1)/(\sigma_{\text{ext,calc}}(q1) + \sigma_{\text{ext,calc}}(q2))$ , where  $\sigma_{\text{ext}}$  is the extinction cross section. The resulting extinction is that due only to singly charged particles. The RI used in the q2 correction is implemented as part of the least squares minimization used to determine the refractive index values in section 3.1, and thus has been determined in a self-consistent manner. The magnitude of the correction was generally largest for the smallest particles due to the initial lognormal particle size distribution peaking around 110–130 nm, which varied somewhat day to day. Additionally, the SMPS measurements allowed for characterization of any particle shrinking due to evaporation following dilution resulting from the addition of the makeup air; in all experiments particle evaporation was negligible (with diameter changes smaller than the resolution of the DMA column).

[10] Within the CRD-AES, the particle stream was split into three flows, one dry and two humidified. The high-RH streams were humidified by passing the aerosol through a temperature-stabilized humidifier before sending the humidified aerosol stream to the CRD cells. It is important to note that in these experiments the humidifiers were maintained at a lower temperature than the CRD cells (typically by 3–5 K) and thus the aerosol was initially exposed to a higher RH than was measured in the cells, usually very close to or at saturation. However, the RH within the two humidified CRD cells was directly measured and was typically ~75% and 85%. The RH was measured using both high-precision Rotronics probes ( $\pm 0.8\%$ ) and lower-precision Vaisala probes ( $\pm 3\%$ ). Both types of probes were calibrated via comparison with saturated salt solutions (using  $\text{MgCl}_2$ , NaCl and KCl) and the RH values were determined with the different probes for the humidified cells agreed to better than 2%. The hygroscopicity of the particles was characterized by measuring the increase in particle extinction in the humidified channels relative to the dry channel, i.e.,  $f_{RH} = \sigma_{\text{ext}}(\text{RH})/\sigma_{\text{ext}}(\text{dry})$ .  $f_{RH}$  has traditionally been used to characterize changes in the scattering coefficient. Note that here  $f_{RH}$  is defined based on extinction measurements, as has been done recently by other authors [Quinn et al., 2005; Baynard et al., 2006; Garland et al., 2007; Beaver et al., 2008; Massoli et al., 2009]; thus, for nonabsorbing particles  $f_{RH}$  from scattering and extinction are equivalent. The  $f_{RH}$  measurements were converted to a single-parameter representation of the particle hygroscopicity by calculating the  $\gamma_{RH}$  value [Gassó et al., 2000; Quinn et al., 2005; Massoli et al., 2009], which is the slope of a linear fit to a plot of  $\log(\sigma_{\text{ext}}(\text{RH}))$  versus  $2 - \log(100 - \text{RH})$ , where RH is in %.

[11] For each OH exposure ( $= [\text{OH}] \times \text{reaction time}$ ) the extinction cross section (units =  $\text{m}^2/\text{particle}$ ) and  $\gamma_{RH}$  were measured for four particle diameters:  $d_p = 130$  nm, 150 nm, 170 nm and 190 nm for squalane and  $d_p = 100$  nm, 120 nm, 150 nm and 190 nm for azelaic acid. For each  $d_p$ -OH exposure pair the extinction coefficient (units =  $1/\text{m}$ ) was measured at various particle concentrations and the  $\sigma_{\text{ext}}$  was determined from a linear fit to a plot of the measured extinction coefficient versus particle number concentration (units =  $\text{particles}/\text{m}^3$ ) [Lack et al., 2006].

[12] OH oxidation lifetime values were determined from the measured OH exposures as

$$\# \text{ of Oxidation Lifetimes} = \tau_{ox} = \frac{[\text{OH}]t}{\tau_k} \quad (1)$$

where  $\tau_k$  is the kinetic lifetime with respect to oxidation ( $1/k$ ) and is given by [Smith et al., 2009]:

$$\tau_k = \frac{4 \cdot \Gamma_{OH} \cdot d_{p,surf} \cdot \rho_0 \cdot N_A}{6 \cdot \bar{c} \cdot MW} \quad (2)$$

where  $\Gamma_{OH}$  is the OH reactive uptake coefficient,  $d_{p,surf}$  is the mean surface-weighted particle diameter,  $\rho_0$  is the particle density,  $N_A$  is Avogadro's number,  $\bar{c}$  is the mean speed of gas phase OH and  $MW$  is the molecular weight.  $[\text{OH}]t$  was determined from the hexane measurements. For a given OH exposure  $\tau_{ox}$  varies inversely with particle diameter. Further, because  $\tau_k$  depends on both MW and density, for a given OH exposure  $\tau_{ox}$  will be different for squalane and azelaic acid. Specifically, for a given OH exposure the  $\tau_{ox}$  for squalane will be 3.4 times greater than for azelaic acid (assuming the same  $\Gamma_{OH}$ ). For squalane, the uptake coefficient has been measured to be 0.3 [Smith et al., 2009]. For azelaic acid, the uptake coefficient is thought to be somewhat larger than squalane and we make the assumption that  $\Gamma_{OH} = 0.5$  for azelaic acid; the exact comparisons presented here will change somewhat if a different  $\Gamma_{OH}$  is used, but the general conclusions are unaffected. Specifically, the relationship between  $\tau_{ox}$  and the magnitude of a given change in one of the measured particle properties, such as that in  $\sigma_{\text{ext}}$  or  $\gamma_{RH}$ , will be altered, but the magnitude of such changes will be unaltered. In calculating  $\tau_{ox}$ , we have made the simplifying assumption that  $\rho_0$ ,  $MW$  and  $d_{p,surf}$  of the distribution are constant [Kroll et al., 2009; Smith et al., 2009]. As such, the calculated  $\tau_{ox}$  are approximate and effectively only account for differences in the selected particle size.

[13] Chemical characterization of organic aerosol is performed using a high-resolution time-of-flight aerosol mass spectrometer (HR-ToF-AMS, Aerodyne Research, Inc.) by methods that we have discussed previously [Kroll et al., 2009; Kessler et al., 2010] and will describe only briefly here. The elemental oxygen-to-carbon and hydrogen-to-carbon ratios (O:C and H:C, respectively) are calculated for the reactive azelaic acid system using the method outlined by Aiken et al. [2007, 2008]. Although the default scaling factors provided for this calculation by Aiken et al. [2008] (0.75 for O:C and 0.91 for H:C) are useful for mixtures containing a variety of components, they are predicted to be less accurate for individual compounds. For this reason, we use a correction factor of 0.26 for O:C and 0.76 for H:C in order to ensure that the preoxidation values match the

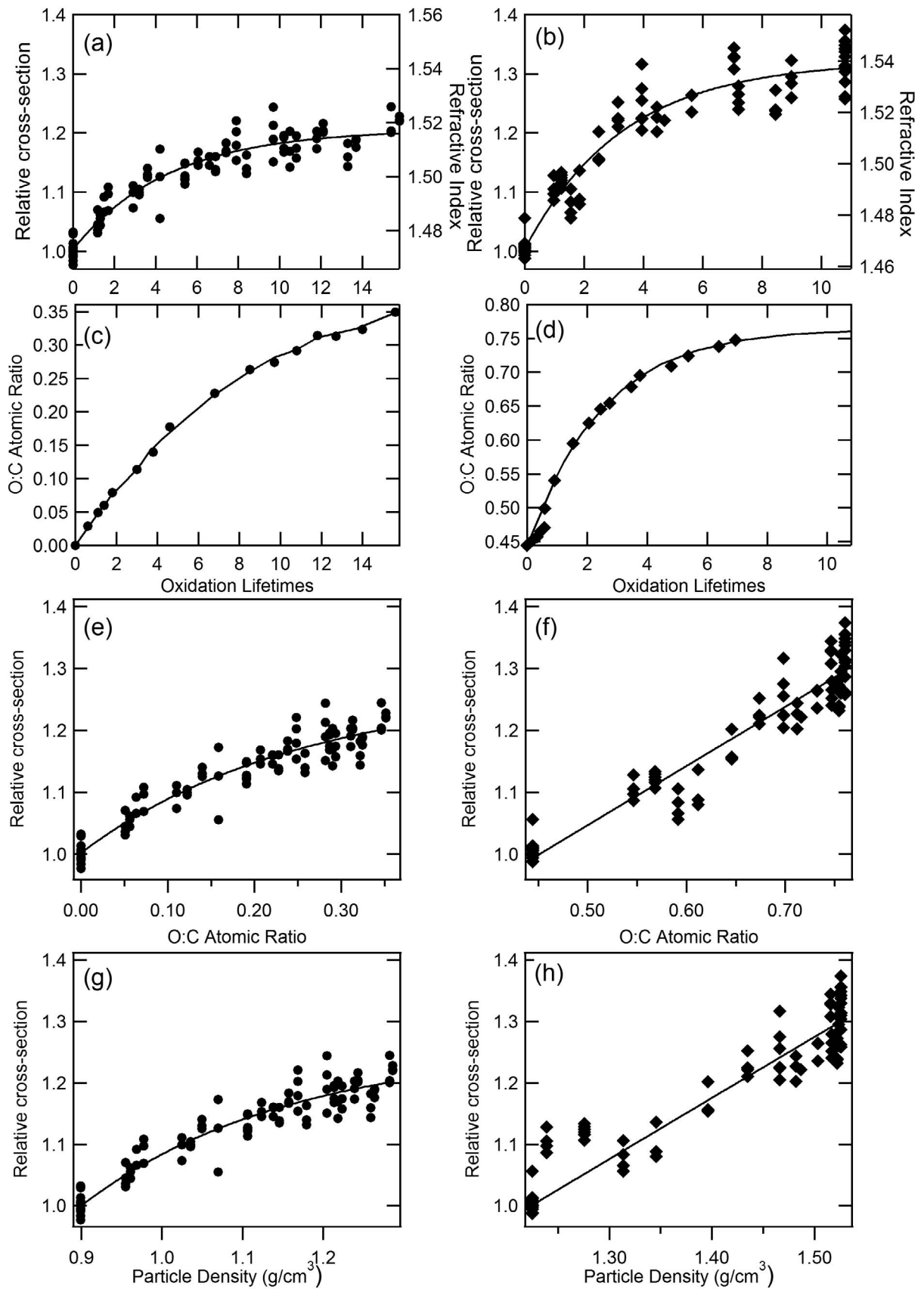


Figure 2

known elemental ratios of pure azelaic acid. Although these factors are unusually low for elemental analysis, the resulting trend of increasing oxygen content with several oxidation lifetimes (Figure 2b) is consistent with previous observations [Kroll *et al.*, 2009].

[14] Particle density, which was observed to change during the course of the experiment, was calculated using the average mobility diameter,  $d_m$  (SMPS); vacuum aerodynamic diameter,  $d_{va}$  (from particle time-of-flight measurements in the AMS); and the standard density,  $\rho_0 = 1 \text{ g cm}^{-3}$ , using the equation:

$$\rho = \frac{d_{va}}{d_m} \rho_0 \quad (3)$$

Minor deviations in particle shape (toward nonspherical geometries) are expected to introduce an error less than 10% [DeCarlo *et al.*, 2004]. It should be noted that the optical/hygroscopicity experiments and composition/density experiments were performed separately and have been connected by relating the  $\tau_{OH}$  values.

### 3. Results and Discussion

#### 3.1. Extinction Cross Section: OH Lifetime

[15] The  $\sigma_{ext}$  values for oxidized squalane and oxidized azelaic acid particles,  $\sigma_{ext}(\tau_{ox})$  relative to the unreacted values,  $\sigma_{ext}(0)$ , have been calculated from the measured extinction coefficients and particle concentrations as  $\sigma_{ext,rel} = \sigma_{ext}(\tau_{ox})/\sigma_{ext}(0)$  (Figures 2a and 2b). An average  $\sigma_{ext}(0)$  for each  $d_p$  has been used as the reference state. As such, the spread observed about the measured  $\sigma_{ext}$  values at zero oxidation lifetimes gives a sense of the measurement reproducibility and precision ( $\pm 3\%$ ,  $2\sigma$ ). This estimate does not account for systematic uncertainties in the particle number concentration measurements; however this should have minimal impact on the relative cross-section measurements because systematic uncertainties in particle number will approximately normalize out in the calculation of  $\sigma_{ext,rel}$ . For both squalane and azelaic acid the measured  $\sigma_{ext,rel}$  values increase with  $\tau_{ox}$ . However, for both compounds the increase in  $\sigma_{ext,rel}$  begins to level out at high OH exposures, with the extinction increasing by  $\sim 20\%$  and  $30\%$  at the highest  $\tau_{ox}$  for the squalane and azelaic acid systems, respectively. The variation in  $\sigma_{ext,rel}$  with  $\tau_{ox}$  showed no distinct dependence on particle size, and thus the different  $d_p$  data have been combined into a single data set. As can be seen in Figure 2, for both compounds the data can be fit to an exponential of the form  $\sigma_{ext,rel}(\tau_{ox}) = y_0(1 - A \cdot \exp[-\tau_{ox}/\tau^*])$ , where  $y_0$ ,  $A$  and  $\tau^*$  are fit constants. The use of an exponential fit does not imply there is a physical basis for this relationship and is only meant as a guide for the eye.

[16] The refractive index of the unreacted squalane and azelaic acid particles can be determined by comparing the measured size-dependent  $\sigma_{ext}$  values with theoretical results from Mie theory (Figure 3) [Bohren and Huffman, 1983;

Lack *et al.*, 2006; Abo Riziq *et al.*, 2007]. Our analysis has been limited to considering only the real part of the refractive index; that is, we assume the particles to be purely scattering. Whether heterogeneous oxidation leads to the formation of absorbing compounds awaits future investigation and the use of direct absorption measurements. Additionally, we assume that the particles are spherical. The best fit RI was determined by minimizing the chi-square value between the q2-corrected measured  $\sigma_{ext}$  and the model  $\sigma_{ext}$ . Both corrected and uncorrected  $\sigma_{ext}$  values are shown in Figure 3, along with the calculated extinction efficiency, which is defined as the actual  $\sigma_{ext}$  divided by the geometric cross section ( $= \pi d_p^2/4$ ). The extinction efficiencies are all less than one due to the relatively small particles used.

[17] The model/measurement comparison yields real RI values of  $n = 1.47 (\pm 0.02)$  for azelaic acid and  $n = 1.47 (\pm 0.02)$  for squalane at 532 nm (Figure 3). Our values are somewhat higher than the literature values azelaic acid (1.430) [Lide, 2006] and slightly higher than that for squalane (1.452) [Sax and Stross, 1957] (these values are presumably for 589.3 nm, the output from a sodium lamp, and not at 532 nm, although this was not explicitly stated in these references). Some of the difference in the azelaic acid refractive index values may derive from the spherical particle assumption employed here. The increase in  $\sigma_{ext}$  that occurs upon oxidation can be considered in terms of a change in the refractive index. Again assuming that the particles are purely scattering, the RI is found to increase to 1.54 for azelaic acid ( $\Delta n = 0.07$ ) and 1.52 for squalane ( $\Delta n = 0.05$ ) for the longest OH exposures, corresponding to the observed 30% and 20% increase in  $\sigma_{ext}$  for azelaic acid and squalane, respectively.

[18] The observed relationship between  $\sigma_{ext}$  (and  $n$ ) and  $\tau_{ox}$  is nonlinear, with  $\sigma_{ext}$  (and  $n$ ) increasing rapidly at first before beginning to plateau at longer times. These results suggest that the optical properties of organic aerosol are not fixed in the atmosphere and that it may be desirable to allow the refractive index for organic aerosol to change as a function of aerosol age within models. However, the measurements presented here only account for heterogeneous oxidation; this is but one pathway by which organic aerosol composition can be modified in the atmosphere. Secondary formation is also important and the evolution of OA optical properties with time should be considered in future studies [Kim *et al.*, 2010].

#### 3.2. Extinction Cross Section: Chemical Composition

[19] It is desirable to determine connections between OA optical properties and chemical composition. One such measurable parameter that can be used is the atomic oxygen-to-carbon and hydrogen-to-carbon ratio. For squalane, the variation in O:C and H:C with OH oxidation lifetime has previously been measured [Kroll *et al.*, 2009; Smith *et al.*, 2009]. The O:C ratio starts at zero for pure squalane and monotonically increases to  $\sim 0.35$  at 17 OH

**Figure 2.** The measured change in the relative extinction cross section and RI are shown as a function of the OH exposure, given as the number of oxidation lifetimes ( $\tau_{ox}$ ), for (a) squalane and (b) azelaic acid. The variation of the O:C atomic ratio versus  $\tau_{ox}$  is shown for (c) squalane and (d) azelaic acid. The change in  $\sigma_{ext,rel}$  is shown as a function of the particle O:C atomic ratio for (e) squalane and (f) azelaic acid. The change in  $\sigma_{ext,rel}$  as a function of particle density for (g) squalane and (h) azelaic acid. Larger densities correspond to longer oxidation lifetimes. In all plots, lines are exponential fits to the data.

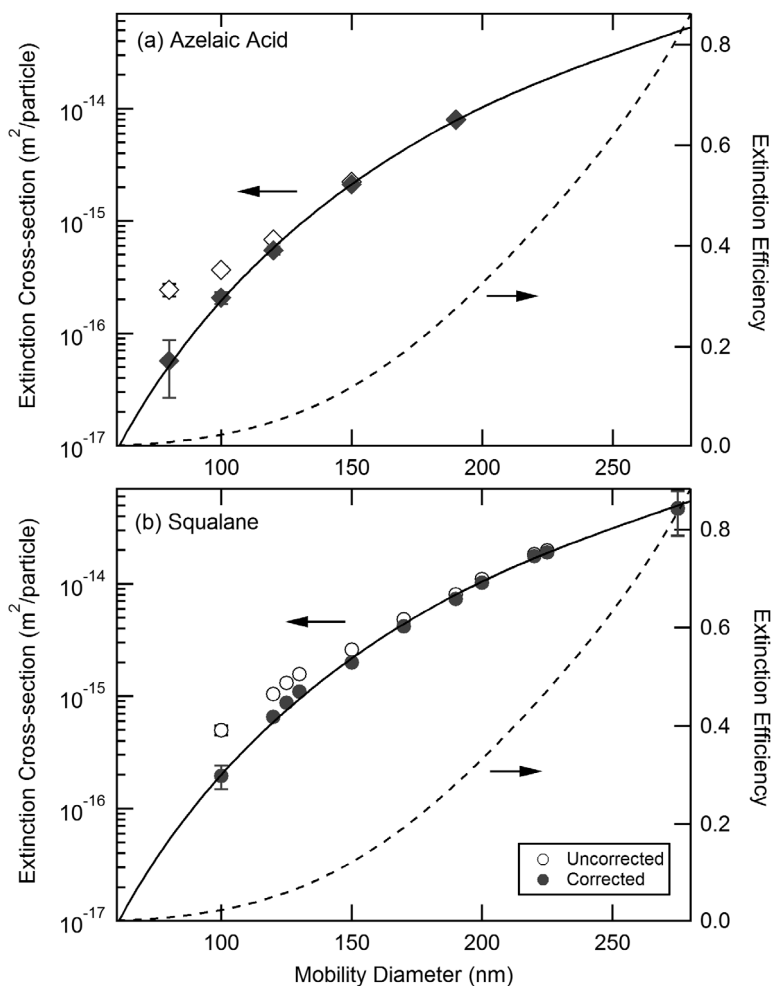


**Figure 3.** Measured extinction cross sections ( $\text{m}^2/\text{particle}$ ) for (a) azelaic acid and (b) squalane as a function of particle diameter. Values are shown for both the raw, uncorrected data (open symbols) and the data after correcting for the influence of multiply charged particles (solid symbols). The solid lines are best fits to the corrected data from Mie theory calculations. Uncertainties in the  $\sigma_{\text{ext}}$  values were obtained as the uncertainties in the slope from a linear fit to extinction versus particle number. The calculated extinction efficiency is shown for reference as a dashed line on the right axis.

oxidation lifetimes while H:C decreases from 2.1 to 1.6 over the same lifetime range. Additionally, particle density is known to increase with oxidation lifetime for the squalane system [Kroll *et al.*, 2009; Smith *et al.*, 2009]. Whereas squalane starts with an O:C = 0, azelaic acid starts with an O:C = 0.44. Note that this value is larger than the maximum reached for squalane via OH oxidation [Kroll *et al.*, 2009; Smith *et al.*, 2009]; as such, oxidized azelaic acid and oxidized squalane particles effectively cover different ranges of O:C. As with squalane, the O:C and particle density for oxidized azelaic acid particles generally increases while the H:C decreases with  $\tau_{\text{ox}}$ .

[20] The functional form of the variation in O:C with  $\tau_{\text{ox}}$  is similar to that observed here for the  $\sigma_{\text{ext}}$  for both the squalane and azelaic acid systems. Thus, it appears that the changing chemical composition of the organic aerosol, in this case through heterogeneous reactions, determines the evolution of the particle real refractive index. Specifically, the addition of oxygen leads to an increase in the real RI (Figure 2c). However, the O:C ratio by itself does not appear

to determine the absolute value of the real RI, as evidenced by the unreacted particles having such similar refractive indices. Other factors, such as particle density, MW, functional group type, etc., must therefore also play a role in determining the real RI. For example,  $\sigma_{\text{ext,rel}}$  (and RI) is also found to increase with the evolving particle density (Figure 2d).

[21] The Lorentz-Lorenz relation (also known as the Clausius-Mossotti relation) relates the refractive index of a substance to the mean polarizability ( $\alpha$ ) and the molecular volume ( $v_m$ ) (or equivalently, density,  $\rho_p$ , divided by molecular weight) of the compound(s) comprising the substance:

$$\frac{(n^2 - 1)}{(n^2 + 2)} = \frac{\alpha}{3 \cdot v_m} = \frac{\rho_p \cdot \alpha}{3 \cdot MW} \quad (4)$$

[22] The refractive indices for the two systems considered in this study (oxidized squalane and azelaic acid) were determined to be very similar, despite the very different

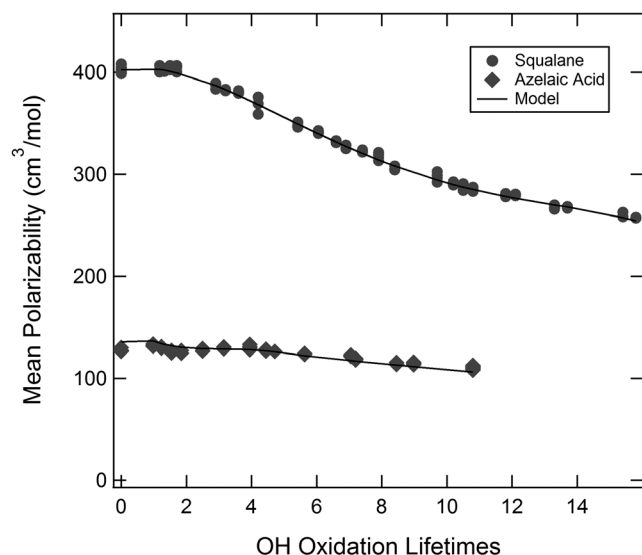


**Figure 4.** The measured mean polarizability is shown for the oxidized squalane (solid circles) and azelaic acid (solid diamonds) systems along with the model fit results (lines). See text for details.

composition of the aerosols. The Lorentz-Lorenz relation indicates that this must result from differences in  $\rho_p$ ,  $MW$  or  $\alpha$  between the two aerosol types. Using our measured refractive index values,  $\alpha$  has been determined for both unreacted aerosol types, with  $\alpha(\text{squalane}) = 410 \text{ cm}^3/\text{mol}$  and  $\alpha(\text{azelaic acid}) = 130 \text{ cm}^3/\text{mol}$ . Thus, a major reason for these two systems having nearly identical refractive index values despite the differences in chemical functionality is that the mean polarizabilities, densities and molecular weights are quite different. If it were assumed, for example, that  $\alpha(\text{squalane}) = \alpha(\text{azelaic acid}) = 130 \text{ cm}^3/\text{mol}$ , then the apparent  $n$  for squalane would be 1.14, which is unrealistically low.

[23] As the squalane and azelaic acid particles are oxidized their chemical composition continuously changes, which leads to a continuous variation in  $n$ ,  $\rho_p$ ,  $MW$ , O:C and H:C and, consequently, in  $\alpha$ . As discussed above, the variation in density of the oxidized squalane and azelaic acid particles is known. We can also estimate how the mean  $MW$  varies with oxidation level from the variation in the absolute elemental composition with  $\tau_{OH}$  [Kroll *et al.*, 2009]. Mean  $MW$  for oxidized squalane increases initially due to functionalization reactions, but eventually fragmentation causes the mean  $MW$  to decrease [Kroll *et al.*, 2009]. Similarly, the mean  $MW$  for oxidized azelaic acid initially increases at low  $\tau_{OH}$  before decreasing at higher  $\tau_{OH}$ . From these observations, the changes in the mean molecular volume ( $v_m = MW/\rho_p$ ) with oxidation have been used to calculate how the mean polarizability varies with  $\tau_{OH}$  for both systems (Figure 4).

[24] The mean polarizability of a mixture is approximately given by the sum of the polarizabilities of the mixture constituents [Feynman *et al.*, 1989; Liu and Daum, 2008]. We postulate that the mean polarizability for organic aerosol can be represented as a weighted linear combination of the

absolute C, O and H elemental abundances, where the weighting factors account for the different polarizabilities and sizes of the constituent atoms:

$$3 \frac{(n^2 - 1)}{(n^2 + 2)} = \frac{\alpha}{v_m} = \sum_i x_i \frac{\alpha_i}{v_{m,i}} = x_C \frac{\alpha_C}{v_{m,C}} + x_H \frac{\alpha_H}{v_{m,H}} + x_O \frac{\alpha_O}{v_{m,O}} = [x_C a_C + x_H a_H + x_O a_O] \quad (5)$$

where  $x_x$  is the mole fraction and  $a_x$  is the weighting factor for the C, O and H atoms that depends on both the polarizability of the individual atoms and the atom-specific molecular volume. Note that the  $a_x$  values are really mean values for the individual atoms since this formulation does not account for differences that might result from the atoms existing with different local environments (e.g., bonding configurations or functional groups). This approach is somewhat similar to that taken by Liu and Daum [2008], except we use atomic composition instead of molecular composition.

[25] If equation (5) is generally valid, then it should be possible to determine a self-consistent set of  $a_C$ ,  $a_H$  and  $a_O$  for both the oxidized squalane and azelaic acid data sets. Using the observational constraints on  $n$ ,  $v_m$  and the  $x_C$ ,  $x_H$  and  $x_O$ , we have used a GRG nonlinear engine (built into Excel 2010) to determine optimal values of  $a_C$ ,  $a_H$  and  $a_O$  by minimizing the “merit function” chi-square ( $\chi^2$ ):

$$\chi^2 = \sum_j \frac{(\alpha_{meas,j} - \alpha_{calc,j})^2}{\varepsilon_{meas,j}^2 + \varepsilon_{calc,j}^2} \quad (6)$$

where the  $\varepsilon$  values are the estimated uncertainties in the measurements and the calculations. (The “measured”  $\alpha$  is the value determined using the RI,  $\rho_p$  and  $MW$  values and the “calculated” the  $\alpha$  from the  $x_x$  and  $a_x$ . The uncertainties in the  $x_x$  were estimated assuming that  $\varepsilon_{O:C}$  and  $\varepsilon_{H:C}$  increase from 10% to 20% over the  $\tau_{ox}$  range considered. The uncertainty in the RI values were  $\pm 0.02$ . The uncertainty in the  $\rho_p$  and  $MW$  were assumed to increase from 5% to 10% over the range of  $\tau_{ox}$  considered. The uncertainties in  $x_x$ ,  $\rho_p$  and  $MW$  were assumed to increase with  $\tau_{ox}$  because we have strong constraints on the values for the unreacted particles.) When the squalane and azelaic acid data sets are combined, the optimization method yields  $a_C = 1.43 \pm 0.11$ ,  $a_H = 0.55 \pm 0.06$  and  $a_O = 0.99 \pm 0.23$ , with the resulting calculated mean  $\alpha$  differing from the measured values by 0.6% and 2.4% on average for the squalane and azelaic acid data sets, respectively. The above uncertainties for the  $a_x$  values were estimated by investigating the variation in the  $\chi^2$  values around the minimized value ( $\chi_0^2$ ), under the assumption that the  $\varepsilon_x$  values are normally distributed. The  $1\sigma$  uncertainty for the  $a_x$  values was determined by finding the  $\chi^2$  that are within one quintile (68.3%) of  $\chi_0^2$ , i.e., the maximum deviations from  $a_x$  for which  $\chi^2 < \chi_0^2 + 3.12$  (the factor of 3.12 comes from there being 3 fitting parameters). The calculated mean  $\alpha$  values are compared to the observations in Figure 4. That both the squalane and azelaic acid data sets can be well represented using a single set of  $a_x$  values suggests that our result may be general.

[26] The values determined here for  $a_O$ ,  $a_H$  and  $a_C$  can, in principle, be used to estimate the ratio  $\alpha/v_m$ , and thus the real refractive index, for any OA system for which O:C and

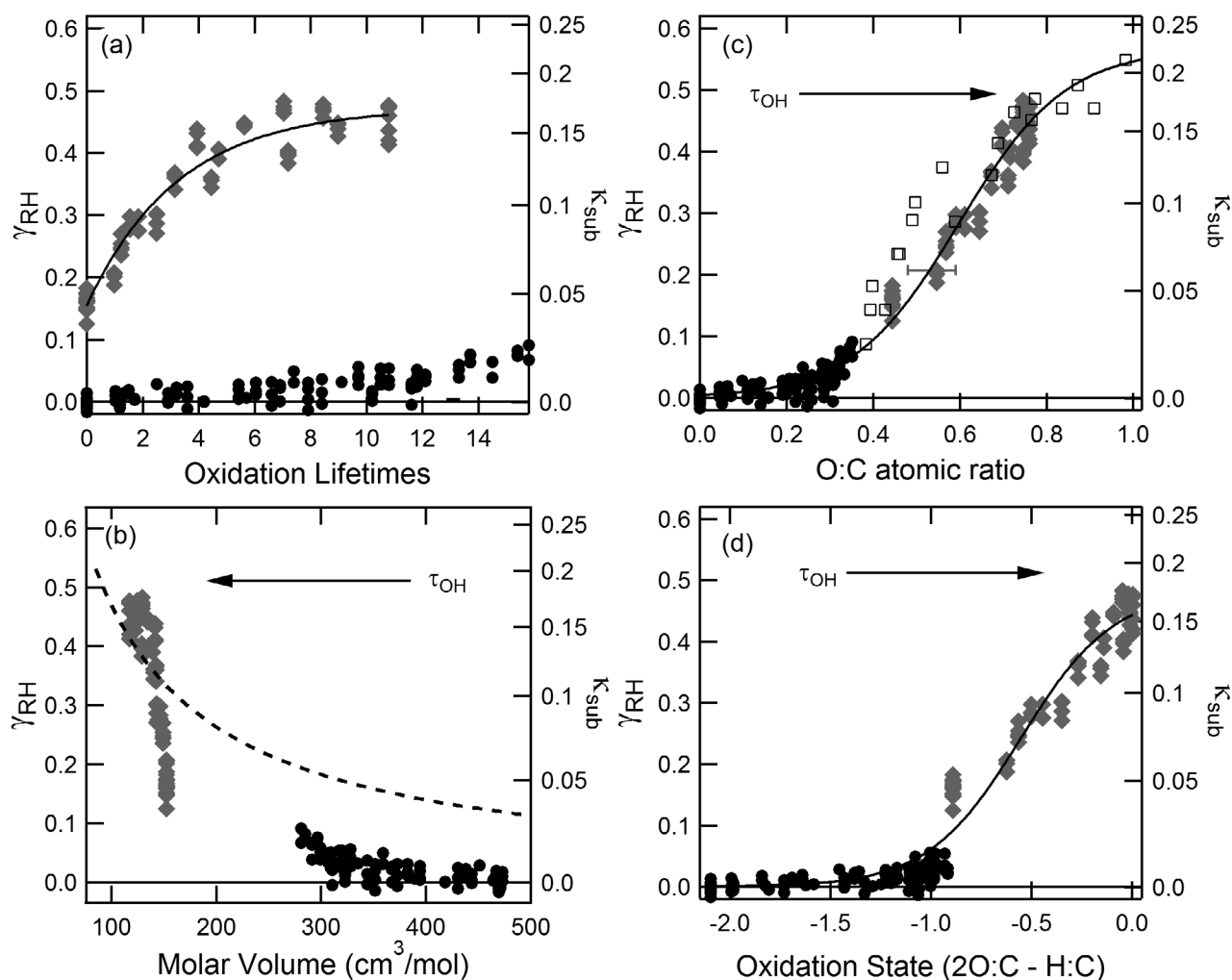


**Figure 5.** The hygroscopicity of organic particles is shown as a function of (a) the oxidation lifetime, (b) molar volume, (c) the O:C atomic ratio, and (d) the average oxidation state,  $2 \times \text{O:C} - \text{H:C}$ , for the squalane (black circles) and azelaic acid (gray diamonds) systems. The solid black line in Figure 5a is a 1-exp fit to the azelaic acid data, while the lines in Figures 5c and 5d are sigmoidal fits to the combined squalane and azelaic acid data sets. Values from lab measurements of *Massoli et al.* [2010] are also shown in Figure 5c as open squares. The dashed line in Figure 5b indicates the intrinsic Raoult's Law hygroscopicity.

H:C are known. We test this idea for the  $\alpha$ -pinene +  $\text{O}_3$  secondary organic aerosol system, for which the evolution of O:C and H:C as a function of mass loading has been previously measured [*Shilling et al.*, 2009]. Using these previous results, the  $\alpha/\nu_m$  for the  $\alpha$ -pinene SOA system are calculated to vary from 0.945 (O:C = 0.3 and H:C = 1.51) to 0.964 (O:C = 0.45 and H:C = 1.38), corresponding to  $n = 1.543$  and 1.556, respectively. Note that because the ratio  $a_{\text{C}}/a_{\text{H}}$  is much larger than  $a_{\text{C}}/a_{\text{O}}$ , the results are particularly sensitive to the measured H:C. These predicted refractive index values are somewhat higher than literature values measured for this same, or similar, chemical systems, which have ranged from 1.41 to 1.53 [*Schnaiter et al.*, 2003; *Barkey et al.*, 2007; *Yu et al.*, 2008; *Kim et al.*, 2010; *Lang-Yona et al.*, 2010; *Nakayama et al.*, 2010]. However, many of these measurements were made at very high mass loadings, where we expect H:C to be relatively large and O:C to

be relatively small [*Shilling et al.*, 2009]. This may be the reason for the overprediction, since high H:C/low O:C conditions would yield a lower  $n$  than calculated above. Further work will be necessary to determine whether the  $a_x$  values given above are generally applicable to organic aerosol. Such investigations can build on the recent finding that O:C and H:C ratios for atmospheric OA are highly correlated [*Heald et al.*, 2010].

### 3.3. Hygroscopicity

[27] As with  $\sigma_{\text{ext,rel}}$ , particle hygroscopicity (i.e.,  $\gamma_{\text{ext}}$ ) was observed to change upon heterogeneous OH oxidation, although the behavior of the squalane and azelaic acid systems were dramatically different (Figure 5). Here, hygroscopicity has been characterized by measuring  $\sigma_{\text{ext}}$  for humidified particles relative to that of dry particles.  $\gamma_{\text{ext}}$  is a single-parameter representation of hygroscopicity and is

independent of absolute RH, unlike  $f_{RH}$  [Quinn *et al.*, 2005; Massoli *et al.*, 2009]. Extinction is typically larger for the humidified particles because water uptake leads to particle growth, which causes the particles to scatter more light per particle compared to the dry particles. This is countered to some extent by the decrease in  $n$  that accompanies water uptake, as water has an RI of 1.33, lower than most organic compounds. However, in general, the effect of particle growth outweighs the decrease in  $n$  such that, overall,  $\sigma_{ext}$  increases.

[28] As expected, it was found that unreacted squalane took up negligible amounts of water at either 75% or 85% RH, with  $\gamma_{RH} = 0 \pm 0.008$ . In contrast, unreacted azelaic acid readily took up water, with  $\gamma_{RH} = 0.162 \pm 0.03$  ( $2\sigma$ ), which corresponds to  $f_{RH} = \sigma_{ext}(85\%RH)/\sigma_{RH}(0\%RH) = 1.36$ . (Note that the reported uncertainties are derived from the experimental precision and do not include uncertainties in the RH measurement, which are  $<2\%$ .) However, previous measurements indicate that the deliquescence RH of azelaic acid is  $>90\%$  [Chan *et al.*, 2008]. One reason that we observe water uptake for azelaic acid at RH  $<90\%$  may be that the RH in our humidifiers was actually 100%. In these studies, the temperature of the humidifiers was  $\sim 3$ – $5$  K less than in the CRD cells. Therefore, given a directly measured RH of 85% at 297 K within the extinction cell, the RH in the humidifier would have been 100% since the dew point is 294 K. As a result, the particles could have deliquesced or activated in the high-RH environment of the humidifiers. If the particles did not effloresce, which seems likely given that the RH remained above 70% in the humidified CRD cells, they would have retained water at the RH at which the  $\gamma_{RH}$  measurements were made. Support for this hypothesis comes from a study by Huff-Hartz *et al.* [2006] who suggested that azelaic acid particles can retain some water after being exposed to high-RH environments (in their case, aerosol generation via atomization). An alternative explanation is that the azelaic acid particles, produced from homogeneous nucleation, actually existed in a supercooled liquid state and did not completely crystallize prior to the  $\gamma_{RH}$  measurement [Bilde and Svenningsson, 2004; Broekhuizen *et al.*, 2004]. If true, this would act to depress the deliquescence RH, and might actually be considered more representative of how ambient OA behaves. Impurities in the particles may have also played a role, although we believe this to be small [Bilde and Svenningsson, 2004; Broekhuizen *et al.*, 2004]. Regardless of the reason for the observed water uptake by the pure azelaic acid particles, our focus is on changes induced via OH oxidation, which have been characterized under constant experimental conditions, and thus our results can be considered in this context.

[29] A weak dependence of  $\gamma_{ext}$  on particle size was observed, with somewhat larger values of  $\gamma_{ext}$  corresponding to smaller  $d_p$  particles. It is known that  $f_{RH}$  values, and consequently  $\gamma_{ext}$  values, can vary nonlinearly with particle size [Baynard *et al.*, 2006; Garland *et al.*, 2007]. The range of variation in the observed  $\gamma_{ext}$  is consistent with theoretical calculations, which indicate that  $\gamma_{ext}$  should decrease somewhat with size for a given growth factor due to the nonlinearity of Mie theory, e.g., from  $\sim 0.18$  (100 nm) to  $\sim 0.14$  (190 nm). Since this size dependence is much smaller than the change in  $\gamma_{ext}$  upon OH oxidation, discussed below, we have chosen to consider the  $\gamma_{ext}$  values as a single data

set, independent of particle size. However, this is likely the reason for some of the spread in the data.

[30] Considering first the azelaic acid particles, as oxidation by OH radicals proceeded the hygroscopicity increased steadily, from 0.16 for unoxidized particles to 0.45 for the highest  $\tau_{ox}$  (Figure 5a). In stark contrast, the hygroscopicity of oxidized squalane particles increases only very slowly with oxidation lifetime (Figure 5a). However, if the  $\gamma_{RH}$  values for both oxidized squalane and azelaic acid particles are plotted together versus their respective O:C values we see that there is continuity between the two model systems and an indication of a sigmoidal relationship between  $\gamma_{RH}$  and O:C (Figure 5c). There is similar continuity between the squalane and azelaic acid data sets and a sigmoidal relationship when  $\gamma_{RH}$  is graphed versus the mean oxidation state,  $\overline{OS}_C$ , calculated as  $2 \times \text{O:C} - \text{H:C}$  [Kroll *et al.*, 2011] (Figure 5d). A sigmoidal relationship indicates that there is an approximate critical threshold for water uptake, with very small values of  $\gamma_{RH}$  being observed when O:C is less than  $\sim 0.25$  or  $\overline{OS}_C$  less than  $-1$ . A sigmoidal fit to the combined oxidized squalane and azelaic acid data yields a plateau of  $\gamma_{ext} \sim 0.57$ . Our results suggest that it may be possible to approximately predict organic aerosol hygroscopicity under subsaturated conditions from O:C or  $\overline{OS}_C$  measurements or vice versa, at least for chemically complex aerosol (for single component particles there is little relationship between O:C and hygroscopicity [Petters *et al.*, 2009]).

[31] A similar relationship between subsaturated particle hygroscopicity and O:C has recently been reported, based on both laboratory secondary organic aerosol growth experiments and field observations [Jimenez *et al.*, 2009; Duplissy *et al.*, 2010; Massoli *et al.*, 2010]. In these studies, hygroscopic growth factors at 95% RH,  $GF(95\%)$ , which is the ratio between the measured  $d_p$  of humidified and dry particles, were measured and reported along with equivalent subsaturated “Kappa” values ( $\kappa_{sub}$ ). Like  $\gamma_{RH}$ ,  $\kappa_{sub}$  is a parameter that describes particle hygroscopicity independent of the measurement RH [Petters and Kreidenweis, 2007]. To facilitate comparison with our measurements, we have converted our  $\gamma_{RH}$  measurements to equivalent  $\kappa_{sub}$  values, as described in Appendix A. There is relatively good agreement between our measurements and the literature results in terms of the shape of the  $\gamma_{RH}$  (or  $\kappa_{sub}$ ) versus O:C relationship, where in Figure 5c we show the  $\kappa_{sub}$  values from the laboratory experiments of Massoli *et al.* [2010]. Thus, the threshold behavior and sigmoidal variation in  $\gamma_{RH}$  (or  $\kappa_{sub}$ ) with O:C appears to be quite general and can potentially be used to parameterize water uptake by organic aerosol under subsaturated conditions [Jimenez *et al.*, 2009; Duplissy *et al.*, 2010; Massoli *et al.*, 2010], although the spread observed among the different measurements suggests that such parameterizations may have significant uncertainties. However, we note that these results may not be generalizable to the estimation of cloud condensation nuclei (CCN) activity (i.e., of supersaturated  $\kappa$  values) as it is known that there are challenges in using subsaturated measurements to predict supersaturated behavior, and vice versa [Prenni *et al.*, 2007; Duplissy *et al.*, 2008; Wex *et al.*, 2009; Massoli *et al.*, 2010].

[32] A few other studies also suggest a link between particle aging, O:C and hygroscopicity (see Figure 5c). For example, Duplissy *et al.* [2008] found that the  $GF(95\%)$  for

$\alpha$ -pinene SOA increased with O:C (as deduced from the m/z 44 fraction measured using an Aerodyne aerosol mass spectrometer) and further that the  $GF(95\%)$  increased as the SOA was aged, and presumably as O:C increased. In a follow-up study, *Jurányi et al.* [2009] observed a similar increase in the  $GF(95\%)$  for  $\alpha$ -pinene SOA with photochemical aging.

[33] There is no theoretically rigorous reason why there should be such a clear relationship between O:C and  $\gamma_{ext}$ . The addition of oxygen to molecules within an aerosol can influence the solubility of the constituent compounds. However, for sufficiently soluble species, particle hygroscopicity is primarily controlled by Raoult's law, with solubility being a secondary concern [Petters and Kreidenweis, 2008]. It is therefore possible that O:C is but one factor, or is serving as a proxy for some other factors, that determine the water uptake behavior. For example, the relationship between  $\gamma_{RH}$  and O:C may be partially controlled by molecular volume changes that accompany changes in the O:C, and not solely by the addition of oxygen [Petters et al., 2009].

[34] Consider that for the squalane system fragmentation of the particle phase molecules during oxidation can be significant and may start to occur at as few as two oxidation lifetimes [Kroll et al., 2009]; some of the particle phase molecules are being broken down into smaller (lower  $v_m$ ) molecules as oxidation progresses. Yet, for this system the addition of oxygen will also be important to the overall hygroscopicity since saturated hydrocarbons are effectively insoluble in water even for small hydrocarbons. For the azelaic acid system, fragmentation is comparably less pronounced upon oxidation, but the increase in density still leads to an overall decrease in  $v_m$ . Yet, azelaic acid is only moderately soluble in water ( $C \sim 4 \times 10^{-3}$  v/v), and thus the observed  $\gamma_{ext}$  for this compound may also be somewhat sensitive to changes in the overall solubility of the particle phase constituents as oxidation progresses [Petters and Kreidenweis, 2008; Petters et al., 2009]. Thus, the relationship between  $\gamma_{ext}$  and O:C for the squalane and azelaic acid systems is likely the result both of an increase in solubility and a decrease in molar volume (or some other property) associated with oxidation. Variations in the O:C ratio appear to capture changes in both properties, at least for the systems under consideration here.

[35] As discussed above, we have observational constraints on how  $v_m$  varies with  $\tau_{OH}$ . Our measurements indicate that, for the chemical systems considered here,  $\gamma_{ext}$  decreases as  $v_m$  increases (Figure 5b). There is a theoretical relationship between  $\kappa$  and  $v_m$  that derives from Raoult's Law assuming an infinitely soluble compound [Petters et al., 2009]. If our observations are compared to this intrinsic limit, it is seen that the squalane results fall far below, as do the less oxidized azelaic acid results, likely as a result of the limited water solubility of the less oxidized compounds comprising the particles. However, at higher  $\tau_{OH}$  values, the azelaic acid system moves toward the intrinsic value, indicating that solubility is becoming less of a constraint. Clearly, the influence of O:C and  $v_m$  on particle hygroscopicity are connected, as these do not vary independently of each other.

[36] As a final note, in the experiments described here we have considered only compounds with H, C and O atoms.

The relationship between O:C (or  $\overline{OS_C}$ ) and  $\gamma_{RH}$  (Figures 5c and 5d) may be sensitive to the presence of other atomic species, specifically, N and S from organic nitrates and sulfates or other N and S containing compounds. Additionally, the azelaic acid particles used here may have existed in a supercooled state (as evidenced by the water uptake by the pure azelaic acid particles), meaning that these results may not be applicable to crystalline organic aerosol. Furthermore, the heterogeneous oxidation likely leads to particles composed of compounds having a distribution of oxygen-containing functional groups (e.g., alcohols, ketones, carboxylic acids, etc.). It may be that particles composed of single compounds behave somewhat differently and do not conform to the relationship found here; as mentioned above, there is no clear relationship between hygroscopicity and O:C for single component aerosol [Petters et al., 2009]. Furthermore, it may be that the complex mixture that is atmospheric OA cannot be well represented as a mixture of just a few (or even many) individual compounds. The more that laboratory OA conforms to the atomic composition of "real" OA [e.g., Heald et al., 2010], the more robust empirical relationships between hygroscopicity and composition likely will be.

#### 4. Conclusions

[37] The evolution of the particle extinction cross sections and the particle hygroscopicity parameter  $\gamma_{ext}$  with exposure to OH radicals has been measured for two model organic aerosol systems, squalane and azelaic acid. It was found that for both systems the  $\sigma_{ext}$  increased continuously with OH exposure, or oxidation lifetime. A 1-exponential relationship between  $\sigma_{ext}$  and  $\tau_{ox}$  was observed, with the  $\sigma_{ext}$  values starting to plateau at long OH lifetimes. The magnitude of the observed changes corresponds to an increase in the particle real refractive index, from 1.48 to 1.55 and from 1.49 to 1.54 for azelaic acid and for squalane, respectively. Relative values of  $\sigma_{ext}$  (normalized to remove the size dependence) were found to increase both with the evolving particle O:C atomic ratio and the particle density. Using the derived RI values, along with the known variation in particle density and an estimated variation in mean MW with oxidation, the variation in the mean polarizability with oxidation was calculated. The calculated mean polarizability was shown to have a relationship with particle chemical composition, specifically with the relative abundances of carbon, hydrogen and oxygen.

[38] These results provide evidence that the optical properties of organic aerosols are not static. On the contrary, they vary with composition, and thus will be expected to depend explicitly on the OA source and the OA age in the atmosphere. By comparing OA optical properties with other physical and chemical properties of OA, it may be possible to eventually develop robust parameterizations that will allow for variation of OA optical properties within models.

[39] Changes to the particle hygroscopicity were also measured as a function of  $\tau_{ox}$ . For azelaic acid, the optical hygroscopicity parameter  $\gamma_{ext}$  increased steadily with increasing  $\tau_{ox}$ . In contrast,  $\gamma_{ext}$  for squalane remained very close to zero until relatively long  $\tau_{ox}$  values were reached. It was shown that the  $\gamma_{ext}$  measurements for azelaic acid and for squalane are connected through the particle O:C ratio or

mean oxidation state,  $\overline{OS}_C$ . For O:C values less than  $\sim 0.25$  (which corresponds to the majority of the squalane oxidation measurements)  $\gamma_{ext}$  remained close to zero. Above O:C = 0.25, the  $\gamma_{ext}$  values increased steadily with increasing O:C, reaching a plateau of  $\gamma_{ext} \sim 0.57$  at high O:C ratios (which corresponds to  $\kappa_{sub} \sim 0.23$ ). Thus, the overall dependence of  $\gamma_{ext}$  on O:C appears to be sigmoidal. In addition, we find that there is a relationship between  $\gamma_{ext}$  and mean molar volume, suggesting that the observed hygroscopicity is a function of both solubility (O:C) and molecule size.

## Appendix A

[40] The conversion of our measured optical hygroscopicity ( $\gamma_{RH}$ ) to equivalent  $\kappa_{sub}$  values was done in a series of steps:

[41] 1. The  $f_{RH}(85\%)$  values were calculated from the measured  $\gamma_{RH}$  as:

$$\ln f_{RH} = \gamma_{RH} \ln \left[ \frac{100 - RH_{ref}}{100 - RH} \right] \quad (A1)$$

where  $RH_{ref} = 0\%$  and  $RH = 85\%$ .

[42] 2. Diameter growth factor ( $GF$ ) values corresponding to the  $f_{RH}$  values were determined for each particle size from Mie theory calculations, where a self-consistent volume weighted refractive index value for the humidified particles was used assuming  $n_{H_2O} = 1.33$  and where  $n_{org}$  was the measured dry value. To do this, first a  $GF$  value was selected and an average refractive index determined using a volume weighting.  $\sigma_{ext}$  was calculated for both the dry particle and the wet particle and from these  $f_{RH}$  was determined. The  $GF$  value was then adjusted until the calculated  $f_{RH}$  equaled the experimental  $f_{RH}(85\%)$ . A unique  $GF$  value is determined for each  $\gamma_{RH}$  using the associated particle diameter as input to the Mie calculations.

[43] 3. The value of  $\kappa_{sub}$  was determined from the  $GF$  values through the relationship [Petters and Kreidenweis, 2007]:

$$\kappa = \frac{GF^3 - 1}{RH/100} \exp \left[ \frac{A}{d_{p,dry} GF} \right] - (GF^3 - 1) \quad (A2)$$

where  $d_{p,dry}$  is the dry particle diameter,  $RH$  is the relative humidity and  $A$  is given as

$$A = \frac{4\sigma_{S/A}M_w}{RT\rho_w} \quad (A3)$$

where  $\sigma_{S/A}$  is the surface tension of water ( $= 0.072 \text{ J}\cdot\text{m}^{-2}$ ),  $M_w$  is the molecular weight of water ( $= 0.018 \text{ kg}\cdot\text{mol}^{-1}$ ),  $R$  is the ideal gas constant,  $T$  is temperature ( $= 298.15 \text{ K}$ ) and  $\rho_w$  is the density of water ( $= 1000 \text{ kg}\cdot\text{m}^{-3}$ ). Like  $\gamma_{ext}$ ,  $\kappa_{sub}$  is a parameter that can be used to describe the hygroscopicity of particles independent of a particular  $RH$  value. However,  $\kappa$  is often used to describe the CCN activity of particles, i.e., the hygroscopicity in the supersaturated regime [Petters and Kreidenweis, 2007]. It is known that there are some challenges in connecting subsaturated  $\kappa$  values ( $\kappa_{sub}$ ) to supersaturated  $\kappa$  values ( $\kappa_{sup}$ ), and thus we emphasize that the values reported here are for the subsaturated regime [Prenni et al., 2007; Duplissy et al., 2008;

Wex et al., 2009; Massoli et al., 2010]. Although the conversion between  $\gamma_{RH}$  and  $GF$  or  $\kappa_{sub}$  is not straightforward (due to the nonlinearity of Mie theory), we nonetheless find that, over the range of  $\gamma_{ext}$  and  $d_p$  values considered in this study, there is an approximately 1-exponential relationship between  $\gamma_{ext}$  and  $\kappa_{sub}$ .

[44] **Acknowledgments.** The authors thank Jared Smith for experimental assistance, Dan Murphy and Dan Lack at NOAA/ESRL/CSD for use of the CRD-AES, Doug Worsnop at Aerodyne for use of the HR-ToF-AMS, and Markus Petters at North Carolina State University for useful discussions. This work was funded by the U.S. National Science Foundation (ATM-0837913) and the U.S. Department of Energy. K.R.W. and portions of this work were supported by the Director, Office of Energy Research, Office of Basic Energy Sciences, Chemical Sciences Division of the U.S. Department of Energy under contract DE-AC02-05CH11231.

## References

- Abo Riziq, A., C. Erlick, E. Dinar, and Y. Rudich (2007), Optical properties of absorbing and non-absorbing aerosols retrieved by cavity ring down (CRD) spectroscopy, *Atmos. Chem. Phys.*, 7(6), 1523–1536, doi:10.5194/acp-7-1523-2007.
- Aiken, A. C., P. F. DeCarlo, and J. L. Jimenez (2007), Elemental analysis of organic species with electron ionization high-resolution mass spectrometry, *Anal. Chem.*, 79(21), 8350–8358, doi:10.1021/ac071150w.
- Aiken, A. C., et al. (2008), O/C and OM/OC ratios of primary, secondary, and ambient organic aerosols with high-resolution time-of-flight aerosol mass spectrometry, *Environ. Sci. Technol.*, 42(12), 4478–4485, doi:10.1021/es703009q.
- Barkey, B., S. E. Paulson, and A. Chung (2007), Genetic algorithm inversion of dual polarization polar nephelometer data to determine aerosol refractive index, *Aerosol Sci. Technol.*, 41(8), 751–760, doi:10.1080/02786820701432640.
- Baynard, T., R. M. Garland, A. R. Ravishankara, M. A. Tolbert, and E. R. Lovejoy (2006), Key factors influencing the relative humidity dependence of aerosol light scattering, *Geophys. Res. Lett.*, 33, L06813, doi:10.1029/2005GL024898.
- Baynard, T., E. R. Lovejoy, A. Pettersson, S. S. Brown, D. Lack, H. Osthoff, P. Massoli, S. Ciciora, W. P. Dube, and A. R. Ravishankara (2007), Design and application of a pulsed cavity ring-down aerosol extinction spectrometer for field measurements, *Aerosol Sci. Technol.*, 41(4), 447–462, doi:10.1080/02786820701222801.
- Beaver, M. R., R. M. Garland, C. A. Hasenkopf, T. Baynard, A. R. Ravishankara, and M. A. Tolbert (2008), A laboratory investigation of the relative humidity dependence of light extinction by organic compounds from lignin combustion, *Environ. Res. Lett.*, 3(4), 045003, doi:10.1088/1748-9326/3/4/045003.
- Bilde, M., and B. Svenningsson (2004), CCN activation of slightly soluble organics: The importance of small amounts of inorganic salt and particle phase, *Tellus, Ser. B*, 56(2), 128–134, doi:10.1111/j.1600-0889.2004.00090.x.
- Bohren, C. F., and D. R. Huffman (1983), *Absorption and Scattering of Light by Small Particles*, 350 pp., John Wiley, New York.
- Broekhuizen, K., P. P. Kumar, and J. P. D. Abbatt (2004), Partially soluble organics as cloud condensation nuclei: Role of trace soluble and surface active species, *Geophys. Res. Lett.*, 31, L01107, doi:10.1029/2003GL018203.
- Chan, M. N., S. M. Kreidenweis, and C. K. Chan (2008), Measurements of the hygroscopic and deliquescence properties of organic compounds of different solubilities in water and their relationship with cloud condensation nuclei activities, *Environ. Sci. Technol.*, 42(10), 3602–3608, doi:10.1021/es7023252.
- DeCarlo, P. F., J. G. Slowik, D. Worsnop, P. Davidovits, and J. L. Jimenez (2004), Particle morphology and density characterization by combined mobility and aerodynamic diameter measurements. Part 1: Theory, *Aerosol Sci. Technol.*, 38, 1185–1205, doi:10.1080/027868290903907.
- Dentener, F., et al. (2006), Emissions of primary aerosol and precursor gases in the years 2000 and 1750 prescribed data-sets for AeroCom, *Atmos. Chem. Phys.*, 6(12), 4321–4344, doi:10.5194/acp-6-4321-2006.
- Dickerson, R. R., S. Kondragunta, G. Stenichkov, K. L. Civerolo, B. G. Doddridge, and B. N. Holben (1997), The impact of aerosols on solar ultraviolet radiation and photochemical smog, *Science*, 278(5339), 827–830, doi:10.1126/science.278.5339.827.
- Duplissy, J., et al. (2008), Cloud forming potential of secondary organic aerosol under near atmospheric conditions, *Geophys. Res. Lett.*, 35, L03818, doi:10.1029/2007GL031075.

- Duplissy, J., et al. (2010), Relating hygroscopicity and composition of organic aerosol particulate matter, *Atmos. Chem. Phys. Discuss.*, 10(8), 19309–19341, doi:10.5194/acpd-10-19309-2010.
- Feynman, R. P., R. B. Leighton, and M. L. Sands (1989), *The Feynman Lectures on Physics*, Addison-Wesley, Redwood City, Calif.
- Fraser, M. P., G. R. Cass, and B. R. T. Simoneit (2003), Air Quality model evaluation data for organics. 6. C<sub>3</sub>–C<sub>24</sub> organic acids, *Environ. Sci. Technol.*, 37(3), 446–453, doi:10.1021/es0209262.
- Garland, R. M., A. R. Ravishankara, E. R. Lovejoy, M. A. Tolbert, and T. Baynard (2007), Parameterization for the relative humidity dependence of light extinction: Organic-ammonium sulfate aerosol, *J. Geophys. Res.*, 112, D19303, doi:10.1029/2006JD008179.
- Gassó, S., et al. (2000), Influence of humidity on the aerosol scattering coefficient and its effect on the upwelling radiance during ACE-2, *Tellus, Ser. B*, 52(2), 546–567, doi:10.1034/j.1600-0889.2000.00055.x.
- Heald, C. L., J. H. Kroll, J. L. Jimenez, K. S. Docherty, P. F. DeCarlo, A. C. Aiken, Q. Chen, S. T. Martin, D. K. Farmer, and P. Artaxo (2010), A simplified description of the evolution of organic aerosol composition in the atmosphere, *Geophys. Res. Lett.*, 37, L08803, doi:10.1029/2010GL042737.
- Huff-Hartz, K. E., J. E. Tischuk, M. N. Chan, C. K. Chan, N. M. Donahue, and S. N. Pandis (2006), Cloud condensation nuclei activation of limited solubility organic aerosol, *Atmos. Environ.*, 40(4), 605–617, doi:10.1016/j.atmosenv.2005.09.076.
- Intergovernmental Panel on Climate Change (2007), *Climate Change: The Physical Science Basis—Contribution of Working Group I to the Fourth Assessment Report of the Intergovernmental Panel on Climate Change*, 996 pp., Cambridge Univ. Press, Cambridge, U. K.
- Jacobson, M. Z. (1999), Isolating nitrated and aromatic aerosols and nitrated aromatic gases as sources of ultraviolet light absorption, *J. Geophys. Res.*, 104(D3), 3527–3542, doi:10.1029/1998JD100054.
- Jimenez, J. L., et al. (2009), Evolution of organic aerosols in the atmosphere, *Science*, 326(5959), 1525–1529, doi:10.1126/science.1180353.
- Jurányi, Z., et al. (2009), Influence of gas-to-particle partitioning on the hygroscopic and droplet activation behaviour of alpha-pinene secondary organic aerosol, *Phys. Chem. Chem. Phys.*, 11(36), 8091–8097, doi:10.1039/b904162a.
- Kanakidou, M., et al. (2005), Organic aerosol and global climate modeling: A review, *Atmos. Chem. Phys.*, 5, 1053–1123, doi:10.5194/acp-5-1053-2005.
- Kessler, S. H., J. D. Smith, D. L. Che, D. R. Worsnop, K. R. Wilson, and J. H. Kroll (2010), Chemical sinks of organic aerosol: Kinetics and products of the heterogeneous oxidation of erythritol and levoglucosan, *Environ. Sci. Technol.*, 44(18), 7005–7010, doi:10.1021/es101465m.
- Kim, H., B. Barkey, and S. E. Paulson (2010), Real refractive indices of  $\alpha$ - and  $\beta$ -pinene and toluene secondary organic aerosols generated from ozonolysis and photo-oxidation, *J. Geophys. Res.*, 115, D24212, doi:10.1029/2010JD014549.
- Kinne, S., et al. (2003), Monthly averages of aerosol properties: A global comparison among models, satellite data, and AERONET ground data, *J. Geophys. Res.*, 108(D20), 4634, doi:10.1029/2001JD001253.
- Kroll, J. H., J. D. Smith, D. L. Che, S. H. Kessler, D. R. Worsnop, and K. R. Wilson (2009), Measurement of fragmentation and functionalization pathways in the heterogeneous oxidation of oxidized organic aerosol, *Phys. Chem. Chem. Phys.*, 11(36), 8005–8014, doi:10.1039/b905289e.
- Kroll, J. H., et al. (2011), Carbon oxidation state as a metric for describing the chemistry of atmospheric organic aerosol, *Nat. Chem.*, 3(2), 133–139, doi:10.1038/nchem.948.
- Lack, D. A., E. R. Lovejoy, T. Baynard, A. Pettersson, and A. R. Ravishankara (2006), Aerosol absorption measurement using photoacoustic spectroscopy: Sensitivity, calibration, and uncertainty developments, *Aerosol Sci. Technol.*, 40, 697–708, doi:10.1080/02786820600803917.
- Lang-Yona, N., Y. Rudich, T. F. Mentel, A. Böhne, A. Buchholz, A. Kiendler-Scharr, E. Kleist, C. Spindler, R. Tillmann, and J. Wildt (2010), The chemical and microphysical properties of secondary organic aerosols from Holm Oak emissions, *Atmos. Chem. Phys.*, 10(15), 7253–7265, doi:10.5194/acp-10-7253-2010.
- Lide, D. R. (2006), *Properties of Organic Compounds*, CRC Press, Boca Raton, Fla.
- Liu, Y. G., and P. H. Daum (2008), Relationship of refractive index to mass density and self-consistency of mixing rules for multicomponent mixtures like ambient aerosols, *J. Aerosol Sci.*, 39(11), 974–986, doi:10.1016/j.jaerosci.2008.06.006.
- Massoli, P., T. S. Bates, P. K. Quinn, D. A. Lack, T. Baynard, B. M. Lerner, S. C. Tucker, J. Brioude, A. Stohl, and E. J. Williams (2009), Aerosol optical and hygroscopic properties during TexAQS-GoMACCS 2006 and their impact on aerosol direct radiative forcing, *J. Geophys. Res.*, 114, D00F07, doi:10.1029/2008JD011604.
- Massoli, P., et al. (2010), Relationship between aerosol oxidation level and hygroscopic properties of laboratory generated secondary organic aerosol (SOA) particles, *Geophys. Res. Lett.*, 37, L24801, doi:10.1029/2010GL045258.
- Murphy, D. M., D. J. Cziczo, K. D. Froyd, P. K. Hudson, B. M. Matthew, A. M. Middlebrook, R. E. Peltier, A. Sullivan, D. S. Thomson, and R. J. Weber (2006), Single-particle mass spectrometry of tropospheric aerosol particles, *J. Geophys. Res.*, 111, D23S32, doi:10.1029/2006JD007340.
- Myhre, G., F. Stordal, T. F. Berglen, J. K. Sundet, and I. S. A. Isaksen (2004), Uncertainties in the radiative forcing due to sulfate aerosols, *J. Atmos. Sci.*, 61(5), 485–498, doi:10.1175/1520-0469(2004)061<0485:UITFRD>2.0.CO;2.
- Nakayama, T., Y. Matsumi, K. Sato, T. Imamura, A. Yamazaki, and A. Uchiyama (2010), Laboratory studies on optical properties of secondary organic aerosols generated during the photooxidation of toluene and the ozonolysis of  $\alpha$ -pinene, *J. Geophys. Res.*, 115, D24204, doi:10.1029/2010JD014387.
- Ng, N. L., et al. (2010), Organic aerosol components observed in Northern Hemispheric datasets from aerosol mass spectrometry, *Atmos. Chem. Phys.*, 10(10), 4625–4641, doi:10.5194/acp-10-4625-2010.
- Petters, M. D., and S. M. Kreidenweis (2007), A single parameter representation of hygroscopic growth and cloud condensation nucleus activity, *Atmos. Chem. Phys.*, 7(8), 1961–1971, doi:10.5194/acp-7-1961-2007.
- Petters, M. D., and S. M. Kreidenweis (2008), A single parameter representation of hygroscopic growth and cloud condensation nucleus activity—Part 2: Including solubility, *Atmos. Chem. Phys.*, 8(20), 6273–6279, doi:10.5194/acp-8-6273-2008.
- Petters, M. D., A. J. Prenni, S. M. Kreidenweis, P. J. DeMott, A. Matsunaga, Y. B. Lim, and P. J. Ziemann (2006), Chemical aging and the hydrophobic-to-hydrophilic conversion of carbonaceous aerosol, *Geophys. Res. Lett.*, 33, L24806, doi:10.1029/2006GL027249.
- Petters, M. D., S. M. Kreidenweis, A. J. Prenni, R. C. Sullivan, C. M. Carrico, K. A. Koehler, and P. J. Ziemann (2009), Role of molecular size in cloud droplet activation, *Geophys. Res. Lett.*, 36, L22801, doi:10.1029/2009GL040131.
- Prenni, A. J., M. D. Petters, S. M. Kreidenweis, P. J. DeMott, and P. J. Ziemann (2007), Cloud droplet activation of secondary organic aerosol, *J. Geophys. Res.*, 112, D10223, doi:10.1029/2006JD007963.
- Quinn, P. K., et al. (2005), Impact of particulate organic matter on the relative humidity dependence of light scattering: A simplified parameterization, *Geophys. Res. Lett.*, 32, L22809, doi:10.1029/2005GL024322.
- Sax, K. J., and F. H. Stross (1957), Squalene: A standard, *Anal. Chem.*, 29(11), 1700–1702, doi:10.1021/ac60131a044.
- Schnaiter, M., H. Horvath, O. Mohler, K. H. Naumann, H. Saathoff, and O. W. Schock (2003), UV-VIS-NIR spectral optical properties of soot and soot-containing aerosols, *J. Aerosol Sci.*, 34(10), 1421–1444, doi:10.1016/S0021-8502(03)00361-6.
- Shilling, J. E., et al. (2009), Loading-dependent elemental composition of alpha-pinene SOA particles, *Atmos. Chem. Phys.*, 9(3), 771–782, doi:10.5194/acp-9-771-2009.
- Smith, J. D., J. H. Kroll, C. D. Cappa, D. L. Che, M. Ahmed, S. R. Leone, D. Worsnop, and K. R. Wilson (2009), The heterogeneous OH oxidation of sub-micron squalene particle: A model system for probing the underlying chemical mechanisms that control aging of ambient aerosols, *Atmos. Chem. Phys.*, 9, 3209–3222, doi:10.5194/acp-9-3209-2009.
- Wex, H., M. D. Petters, C. M. Carrico, E. Hallbauer, A. Massling, G. R. McMeeking, L. Poulain, Z. Wu, S. M. Kreidenweis, and F. Stratmann (2009), Towards closing the gap between hygroscopic growth and activation for secondary organic aerosol: Part 1—Evidence from measurements, *Atmos. Chem. Phys.*, 9(12), 3987–3997, doi:10.5194/acp-9-3987-2009.
- Yu, Y., M. J. Ezell, A. Zelenyuk, D. Imre, L. Alexander, J. Ortega, B. D'Anna, C. W. Harmon, S. N. Johnson, and B. J. Finlayson-Pitts (2008), Photooxidation of alpha-pinene at high relative humidity in the presence of increasing concentrations of NO<sub>x</sub>, *Atmos. Environ.*, 42(20), 5044–5060, doi:10.1016/j.atmosenv.2008.02.026.
- Zhang, Q., et al. (2007), Ubiquity and dominance of oxygenated species in organic aerosols in anthropogenically influenced Northern Hemisphere midlatitudes, *Geophys. Res. Lett.*, 34, L13801, doi:10.1029/2007GL029979.

C. D. Cappa, Department of Civil and Environmental Engineering, University of California, Davis, CA 95616, USA. (cdcappa@ucdavis.edu)

D. L. Che, Department of Chemistry, Stanford University, Stanford, CA 94305, USA.

S. H. Kessler and J. H. Kroll, Department of Chemical Engineering, Massachusetts Institute of Technology, Cambridge, MA 02139, USA.

K. R. Wilson, Chemical Sciences Division, Lawrence Berkeley National Laboratory, Berkeley, CA 94720, USA.